

## ELECTRONIC STRUCTURES OF PRECIPITATE-HARDENING PHASES IN ALUMINIUM ALLOYS

M.KISHIMOTO, H.YUKAWA and M.MORINAGA

Department of Materials Science and Engineering,  
Graduate School of Engineering, Nagoya University,  
Furo-cho, Chikusa-ku, Nagoya 464-8603, JAPAN  
Phone: +81 52 789 4638, Fax: +81 52 789 4202  
e-mail: morinaga@numse.nagoya-u.ac.jp

**ABSTRACT** The electronic structures are calculated of four principal precipitate-hardening phases,  $\text{Al}_2\text{Cu}$ ,  $\text{Mg}_2\text{Si}$ ,  $\text{MgZn}_2$  and  $\text{Al}_3\text{Li}$  in aluminium alloys by the DV-X $\alpha$  cluster method. It is found that nearly-free electrons behavior is observed in  $\text{Al}_3\text{Li}$ . On the other hand, a sort of covalent interaction seems operating partially in  $\text{Mg}_2\text{Si}$  in addition to the ionic interaction due to the charge transfer between Mg and Si atoms. Although there are directional interactions between Cu atoms in  $\text{Al}_2\text{Cu}$ , and between Zn atoms in  $\text{MgZn}_2$ , they are considered to be intermediate between  $\text{Al}_3\text{Li}$  and  $\text{Mg}_2\text{Si}$  from a view of the nature of chemical bond between atoms in them.

**Keywords :** *aluminium alloys, electronic structures, DV-X $\alpha$  cluster method, precipitate hardening, chemical bond*

### 1. INTRODUCTION

The electronic structures of aluminium alloys have been calculated by many investigators [1,3]. For example, an electronic approach has been proposed to the prediction of mechanical properties of aluminium alloys [4]. Needless to say, the types of precipitate-hardening phases are important in understanding mechanical properties of high-strength alloys. The main precipitate-hardening phases are  $\theta(\text{Al}_2\text{Cu})$ ,  $\beta(\text{Mg}_2\text{Si})$ ,  $\eta(\text{MgZn}_2)$  and  $\delta'(\text{Al}_3\text{Li})$  phase in the 2000-, 6000-, 7000 and Al-Li series aluminium alloys, respectively.

Recently, we have found that the average number of valence electrons per atom, ( $e/a$ ) of the precipitates correlates well with the maximum tensile strength of each alloy as shown in Fig.1. It is supposed that the search for new precipitate with the ( $e/a$ ) value less than 2 is indeed needed to develop high-strength alloys of having the tensile strength more than 700 MPa. For this purpose, it is firstly important in understanding characteristics of each precipitate phase in a fundamental manner.

In this study, the electronic structures of four

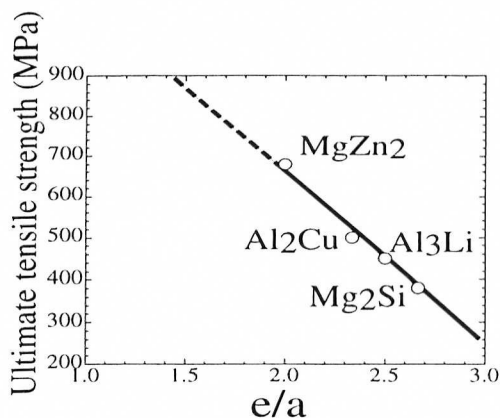


Fig.1 Relationship between maximum ultimate tensile strength and ( $e/a$ ).

precipitates are calculated by the DV-X $\alpha$  cluster method. The crystal structures of intermediate phases which appear in the course of aging at low temperatures are not known, so that the present calculations are performed for their equilibrium precipitate phases.

# 2. DV-X $\alpha$ CLUSTER METHOD AND CLUSTER MODELS

The DV-X $\alpha$  cluster method is one of the molecular orbital methods, assuming a Slater's X $\alpha$  exchange correlation potential. The parameter  $\alpha$  is fixed at 0.7, an empirically appropriate value, and the self-consistent charge approximation is used in the calculation. The matrix elements of the Hamiltonian and the overlap

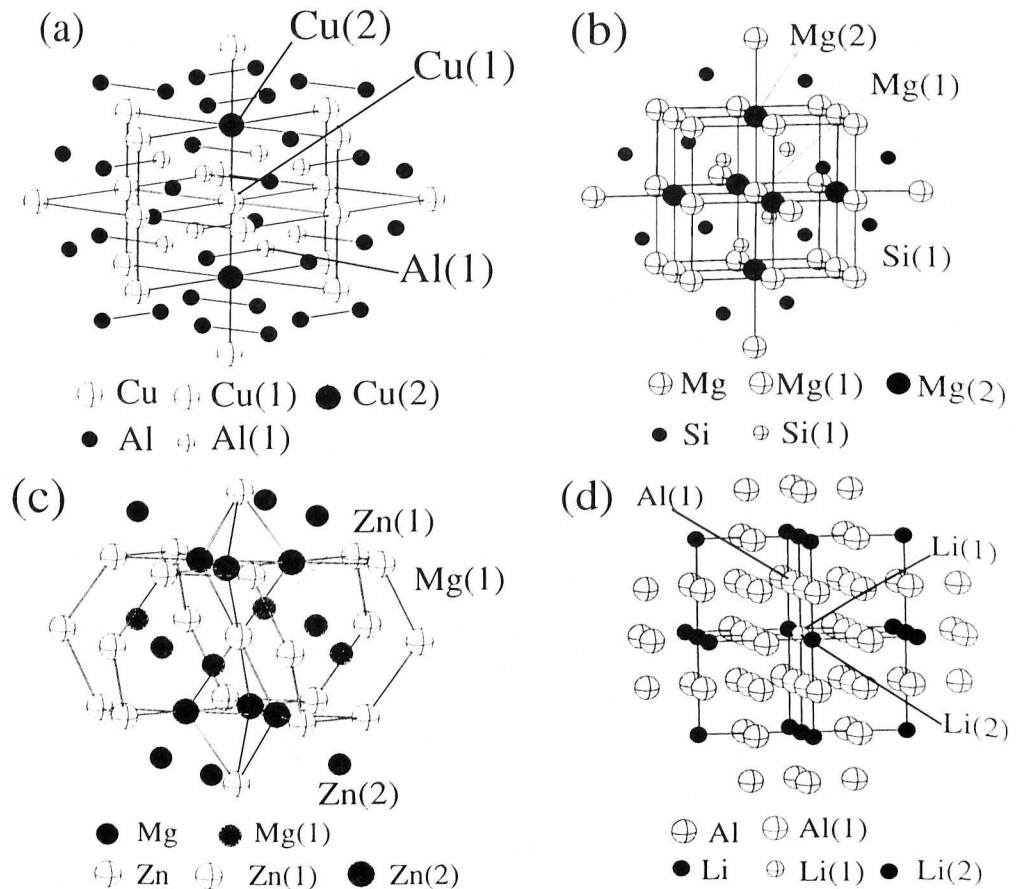


Fig.2 Cluster models used in the calculation; (a)  $\text{Al}_{40}\text{Cu}_{21}$  cluster for  $\text{Al}_2\text{Cu}$ , (b)  $\text{Mg}_{33}\text{Si}_{16}$  cluster for  $\text{Mg}_2\text{Si}$ , (c)  $\text{Mg}_{12}\text{Zn}_{27}$  cluster for  $\text{MgZn}_2$ , and (d)  $\text{Al}_{60}\text{Li}_{19}$  cluster for  $\text{Al}_3\text{Li}$ .

Table 1 Interatomic distances in precipitate phases (nm)

$\text{Al}_2\text{Cu}$		$\text{Mg}_2\text{Si}$		$\text{MgZn}_2$		$\text{Al}_3\text{Li}$	
Cu(1)-Cu(2)	0.2439	Mg(1)-Mg(2)	0.3173	Zn(1)-Zn(2)	0.2633	Li(1)-Al(1)	0.2835
Cu(1)-Al(1)	0.2590	Mg(1)-Si(1)	0.2748	Zn(1)-Mg(1)	0.3062	Al(1)-Al(2)	0.2835
Al(1)-Al(2)	0.2713	pure Mg	0.3191	pure Mg	0.3191	pure Al	0.2863
pure Al	0.2863	pure Si	0.2347	pure Zn	0.2913	pure Li	0.2758
pure Cu	0.2556						

integrals are calculated by the random sampling method. The molecular orbitals are constructed by a linear combination of numerically generated atomic orbitals; 1s-4p for 3d transition elements, 1s-5p for 4d transition elements, 1s-3d for Al and Si and 1s-4d for Ga and Ge. The detailed explanation of the calculation method is given elsewhere [5,7].

The cluster models of  $\text{Al}_{40}\text{Cu}_{21}$ ,  $\text{Mg}_{33}\text{Si}_{16}$ ,  $\text{Mg}_{12}\text{Zn}_{27}$ ,  $\text{Al}_{60}\text{Li}_{19}$  are constructed according to the respective crystal structures as shown in Fig.2(a)-(d) [8]. The interatomic distances are listed in Table 1, together with the first-nearest-neighbor interatomic distances of pure metals. The atom symbols used in Table 1 (e.g., Cu(1)) are the same ones shown in Fig.2(a)-(d). These cluster models are chosen so that its composition ratio in the cluster is close to that of each precipitate.

### 3. RESULTS AND DISCUSSION

#### 3.1 Electron density of states

The electron density of states is shown in Fig.3 (a), (b), (c) and (d), for  $\text{Al}_2\text{Cu}$ ,  $\text{Mg}_2\text{Si}$ ,  $\text{MgZn}_2$  and  $\text{Al}_3\text{Li}$  phase respectively. The Fermi energy level,  $E_f$ , is indicated by an arrow in each figure. As shown in (a) for  $\text{Al}_2\text{Cu}$ , Al 3s and 3p components spread near the  $E_f$ , even though Cu 4s and 4p components still exist near the  $E_f$ . Also, for  $\text{Mg}_2\text{Si}$ , both the Mg 3s, 3p and Si 3s, 3p components extend over the wide energy range as shown in (b). Similarly, the electron density of states for  $\text{MgZn}_2$  shown in (c) resembles that for  $\text{Al}_2\text{Cu}$  shown in (a). Furthermore, as shown in (d) for  $\text{Al}_3\text{Li}$ , it changes in an approximately parabolic way with respect to the energy, indicating that the electrons behave nearly-freely in this phase. This is reasonable since both Al and Li atoms are simple s, p metals.

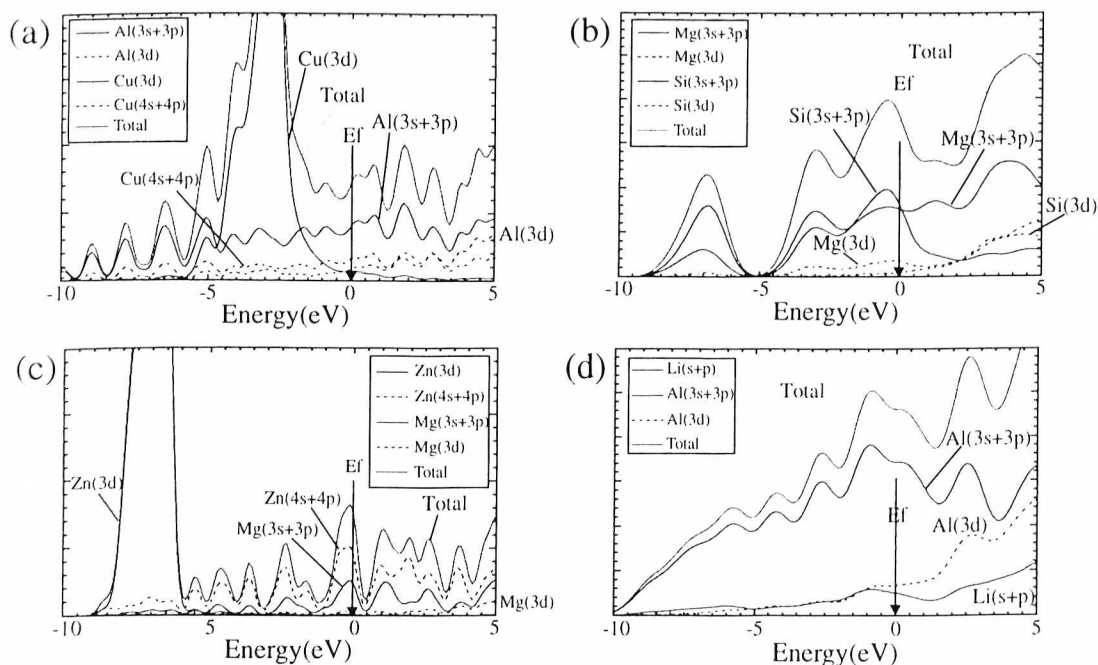


Fig.3 Total and partial electron densities of states for (a)  $\text{Al}_2\text{Cu}$ , (b)  $\text{Mg}_2\text{Si}$ , (c)  $\text{MgZn}_2$  and (d)  $\text{Al}_3\text{Li}$ .

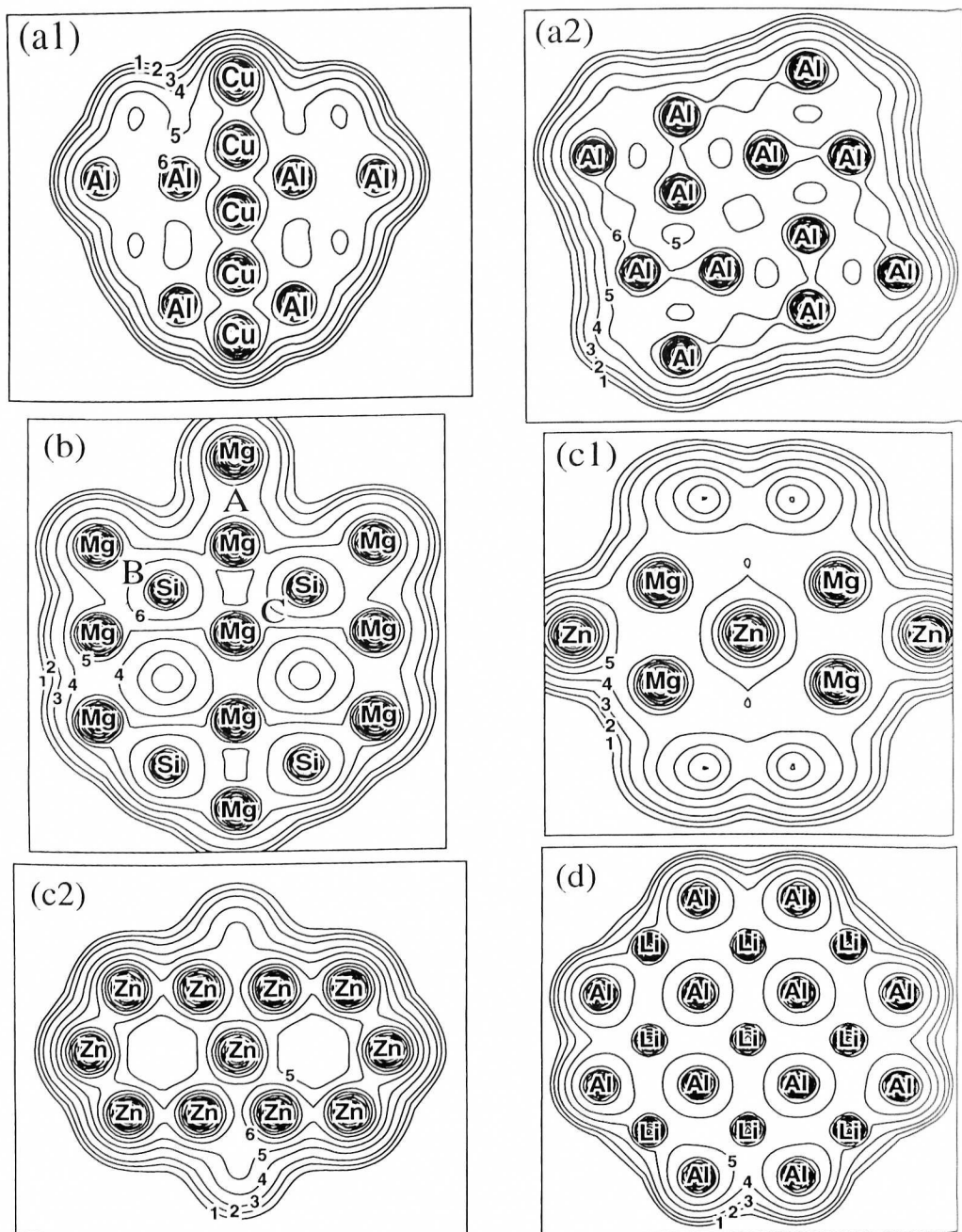


Fig.4 Contour maps of the electron density distributions; (a1) the (360) atomic plane and (a2) the (002) atomic plane in  $\text{Al}_2\text{Cu}$ , (b) the (110) atomic plane in  $\text{Mg}_2\text{Si}$ , (c1) the atomic plane containing both Mg atoms and Zn atoms and (c2) the atomic plane containing only Zn atoms in  $\text{MgZn}$  and (d) the (001) atomic plane in  $\text{Al}_3\text{Li}$ . The denoted numbers, 1,2,3,4,5 and 6 correspond to the electron density values, 0.005, 0.01, 0.02, 0.04, 0.08 and 0.16 (in electrons per cube of the atomic unit), respectively (1 a.u.=0.0529nm).

### 3.2 Spatial electron density distributions

The spatial electron density distributions are shown in Fig.3(a1)-(d) for the four precipitates. For  $\text{Al}_2\text{Cu}$ , as shown in (a1), strong directional interactions are operating between Cu atoms aligned along the [001] direction. In response to this, the Cu(1)-Cu(2) interatomic distance, 0.2439 nm, is much shorter in this phase than that in pure Cu, 0.2556 nm. Similarly, as shown in (a2), strong interactions are operating between Al atoms. Their interatomic distance is 0.2713 nm, shorter than that in pure Al, 0.2863 nm.

For  $\text{Mg}_2\text{Si}$ , the spatial electron density is spread between Mg and Si atoms, as each atom is indicated by A for Mg and B for Si in the figure (b). This implies that a sort of covalent interaction seems operating between them. On the other hand, such a strong interaction is not present between Mg atoms as indicated by A and C in the figure. This may be understood from their interatomic distance, 0.3173 nm, comparable to that in pure Mg, 0.3191 nm.

For  $\text{MgZn}_2$ , as shown in (c1), the electron densities around a central Zn atom and also around the surrounding Mg atoms seem to be less extended on this atomic plane. This probably means that the interaction is weak between Mg and Zn atoms. This is also the case between Mg atoms. However, as shown in (c2), Zn atoms form a hexagon and they interact rather strongly with each other. Thus, more important is this Zn-Zn interaction in  $\text{MgZn}_2$ , as might be expected from the fact that the Zn-Zn interatomic distance of this phase, 0.2633 nm, is much shorter than that of pure Zn, 0.2913 nm.

Finally for  $\text{Al}_3\text{Li}$ , as shown in (d), all the interactions may not be strong between Al atoms, between Li atoms, and between Al and Li atoms. This is because, the electron density distributions around each atom are spherical without showing any directional distributions in it.

### 3.3 Ionicity of atoms and charge transfer

In order to investigate the charge transfer between atoms, the ionicity of each atom is estimated following the Mulliken population analysis. The charge transfer takes place between the central atom in the cluster (e.g., Cu(1) in the  $\text{Al}_2\text{Cu}$  cluster) and the surrounding atoms (e.g., Al(1)), as is illustrated in Fig.5. In case of  $\text{Al}_2\text{Cu}$ , it occurs from Al(1) atom to Cu(1) atom. The amount of transferred charges changes in the order,  $\text{Mg}_2\text{Si} > \text{Al}_2\text{Cu} > \text{MgZn}_2 > \text{Al}_3\text{Li}$ . Thus,  $\text{Mg}_2\text{Si}$  is a compound of having a covalent interaction as well as the ionic interaction due to the charge transfer between atoms. This is reflected on the highest melting temperature, 1358 K, of  $\text{Mg}_2\text{Si}$  among the four precipitates. By contraries,  $\text{Al}_3\text{Li}$  is a compound of having weak atomic interactions and its solvus temperature is as low as 613 K.

## 4. CONCLUSION

The electronic structures of precipitate-hardening phases in aluminium alloys are investigated by the DV- $X\alpha$  cluster method. Nearly-free electrons behavior is observed in the electronic structure of  $\text{Al}_3\text{Li}$ , even though charge transfer takes place slightly from Al atom to Li atom in it. On the other hand, in case of  $\text{Mg}_2\text{Si}$ , a sort of covalent interaction seems operating in addition to the ionic interaction

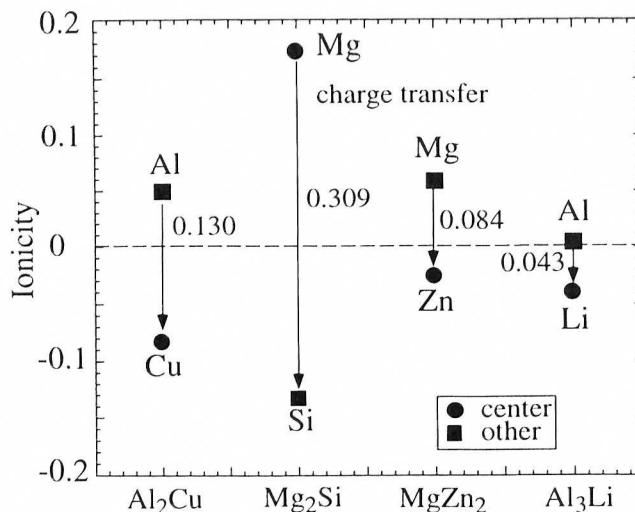


Fig.5 Ionicities of a central atom in the cluster and the surrounding atoms. The difference in the ionicity between them represents the amount of transferred charges between atoms.

due to the considerable charge transfer from Mg atom to Si atom. Both  $\text{Al}_2\text{Cu}$  and  $\text{MgZn}_2$  are intermediate between  $\text{Al}_2\text{Cu}$  and  $\text{Mg}_2\text{Si}$  in view of the nature of chemical bond between atoms.

## ACKNOWLEDGMENTS

The authors acknowledge the Computer Center, Institute for Molecular Science, Okazaki National Institutes for the use of the SX-3/34 R computer. This research was supported by Grant-in-Aid for Scientific Research from the Ministry of Education, Science, Sports and Culture of Japan.

## REFERENCES

- [1] B.Segall: Phys. Rev., 124 (1961), 1797
- [2] M.Manninen, P.Jena, R.M.Nieminen and J.K.Lee: Phys. Rev., B24 (1981), 7057
- [3] M.Morinaga, S.Nasu, H.Adachi, J.Saito and N.Yukawa: J.Phys.: Condens. Matter, 3 (1991), 6817
- [4] M.Morinaga, S.Kamado: Model. Simul. Mater. Sci. Eng. 1 (1993), 151
- [5] J.C. Slater, Quantum Theory of Molecules and Solids, McGraw-Hill, New York, 1974
- [6] E. D. Ellis and G. S. Painter, Phys. Rev., 82 (1970), 2887
- [7] H. Adachi, M. Tsukada and C.Satoko: J.Phys. Soc. Jpn., 45 (1978), 490
- [8] P. Villars: Pearson's Handbook Desk Edition of Crystallographic Data for Intermetallic Phases, Vol.1,2,(1997)